

## Fluid model of the boundary of a one-dimensional plasma under the influence of an oblique magnetic field for a wide range of collisionality

T. M. G. Zimmermann, M. Coppins, and J. E. Allen

Citation: [Physics of Plasmas \(1994-present\)](#) **15**, 072301 (2008); doi: 10.1063/1.2946436

View online: <http://dx.doi.org/10.1063/1.2946436>

View Table of Contents: <http://scitation.aip.org/content/aip/journal/pop/15/7?ver=pdfcov>

Published by the [AIP Publishing](#)

---

### Articles you may be interested in

[Sheath and boundary conditions in a collisional magnetized warm electronegative plasma](#)

Phys. Plasmas **20**, 063503 (2013); 10.1063/1.4811479

[Boundary conditions for plasma fluid models at the magnetic presheath entrance](#)

Phys. Plasmas **19**, 122307 (2012); 10.1063/1.4771573

[Properties of a warm plasma collisional sheath in an oblique magnetic field](#)

Phys. Plasmas **19**, 113504 (2012); 10.1063/1.4766476

[A two-dimensional hybrid model of the Hall thruster discharge](#)

J. Appl. Phys. **100**, 023304 (2006); 10.1063/1.2219165

[Kinetic analysis of the plasma boundary layer in an oblique magnetic field](#)

Phys. Plasmas **6**, 2409 (1999); 10.1063/1.873512

---

Did your publisher get  
**18 MILLION DOWNLOADS** in 2014?  
AIP Publishing did.



THERE'S POWER IN NUMBERS. Reach the world with AIP Publishing.



# Fluid model of the boundary of a one-dimensional plasma under the influence of an oblique magnetic field for a wide range of collisionality

T. M. G. Zimmermann,<sup>1,a)</sup> M. Coppins,<sup>1</sup> and J. E. Allen<sup>1,2</sup>

<sup>1</sup>Blackett Laboratory, Imperial College, Prince Consort Road, London SW7 2BW, United Kingdom

<sup>2</sup>University College, Oxford, OX1 4BH, United Kingdom

(Received 25 January 2008; accepted 27 May 2008; published online 8 July 2008)

The effect of a magnetic field on the boundary of a plasma is studied using a one-dimensional fluid model based on the work of K.-U. Riemann [Contrib. Plasma. Phys. **34**, 127 (1994)]. The model takes into account the effects of both collisions and ionization. Two limiting regimes are identified: the collisional presheath and the (highly) magnetized presheath. Results from this model demonstrate that a highly magnetized presheath may be treated in terms of two regions: The **B**-aligned presheath and a Chodura layer [R. Chodura, Phys. Fluids **25**, 1628 (1982)]. The properties of this Chodura layer are explored in some detail and it is found that the size of this layer, for example, follows a simple expression in the highly magnetized regime. Finally, an attempt is made to recover the singular behavior of the Chodura layer as the magnetic field becomes very strong and use a pseudo two-scale approach to resolve both scale lengths of the magnetized presheath. © 2008 American Institute of Physics. [DOI: [10.1063/1.2946436](https://doi.org/10.1063/1.2946436)]

## I. INTRODUCTION

The interaction of a plasma with a solid object (most often the confining vessel) is a problem almost as old as plasma physics itself. Pioneering work regarding the plasma boundary was due to Langmuir, who defined the terms “sheath”<sup>1</sup> and “plasma”<sup>2</sup> in 1923 and 1928, respectively. The relevant quotations are given in Ref. 3, a topical review by Franklin, which also includes a discussion of the transition layers between plasma and boundary. More recently, the boundary of a magnetized plasma has been treated by Franklin<sup>4</sup> and Cetiner.<sup>5</sup> Despite prolonged investigation, interest in the field has not diminished. If anything, plasma boundary physics has drawn even more attention in recent years due to its relevance to materials processing, plasma diagnostics (Langmuir probes, for example), and magnetic confinement fusion. An understanding of the structure of the transition between plasma and solid is crucial to predict production yields, interpret measurements, or assess the sustainability of the plasma itself. The boundary of a magnetized plasma poses a particularly interesting problem, provided the magnetic field is not perpendicular to the wall. Transport of ions to the wall is now inhibited, which has to be taken into account if the Bohm criterion is to be fulfilled at the sheath edge. One can think of several different applications where one encounters magnetic fields at the plasma boundary, but the divertor/limiter of a magnetic confinement fusion reactor is perhaps the most obvious. Here, the magnetic field makes a variety of angles with the surface, from near perpendicular to grazing and it is certainly strong enough to influence the ion motion.

In the simplest case, one considers a stationary plasma, which is brought into contact with a completely absorbing boundary. Under most conditions, the electron time scale is far shorter than that of the ions. This means that the wall is

bombarded with electrons before the ions can react and thus acquires a negative charge. The ions respond to the potential formed by this charge and are accelerated towards the boundary. Once the system has settled into a steady state one can identify two regions: the quasineutral presheath and a region of positive space charge called the sheath. The former adopts the scale length of whatever process dominates the ion motion. Alternatively, it can be determined by the size of the vessel to which the plasma is confined, in which case one must solve for the appropriate plasma parameters. The sheath is usually several Debye lengths wide, which is perhaps to be expected as its function is to shield the plasma from the negatively charged wall.

It is common practice to use two-scale theory<sup>6</sup> when modelling the plasma boundary. Applicability of the two scale approach hinges on the assumption that the Debye length is vanishingly small compared to all other length scales of interest. The plasma boundary problem can then be split into a presheath and a sheath solution, which are found separately. Working on two physically and mathematically independent scales greatly simplifies the problem, since different assumptions can be made about each region. For example, it is usually assumed that there are no collisions (including ionizing collisions) in the sheath. The collisionality of the presheath varies from model to model. This has a curious effect on the width of presheath and sheath on the two length scales (Fig. 1). When working on the sheath scale, the presheath begins at a point which is infinitely far away from the solid wall; the sheath is effectively infinite. On the presheath scale, however, the sheath is infinitesimally small and directly adjacent to the wall. Due to this behavior one encounters severe difficulties in matching<sup>3,7</sup> the solution obtained on either scale into a continuous transition from bulk plasma to wall.

At the singular point, from hereon referred to as the sheath edge, the ion fluid has to fulfill the so-called “Bohm

<sup>a)</sup>Electronic mail: tassilo.zimmermann02@imperial.ac.uk.

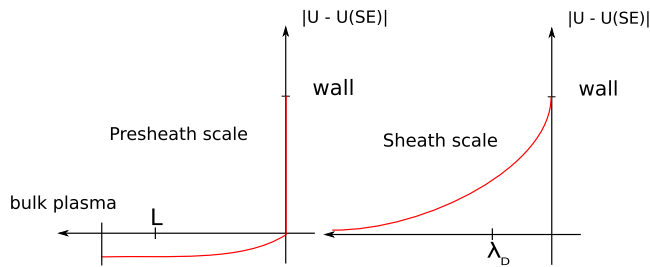


FIG. 1. (Color online) Magnitude of the electrostatic potential,  $U$ , across the plasma boundary. On the presheath scale, the sheath is infinitely thin while on the sheath scale the sheath edge is infinitely far from the wall (since the sheath is usually treated as quiescent).

criterion.” This relates to the fact that the sheath is constantly losing ions to the boundary, which need to be replaced by ions drawn from the presheath. This criterion was already present in the work of Langmuir,<sup>1,2,8</sup> but was first stated explicitly by Bohm;<sup>9</sup> hence the name. There also exists a kinetic equivalent of the Bohm criterion, due to Harrison and Thompson,<sup>10</sup> which places a condition on the distribution function of the ions.

Early work on the magnetized plasma boundary by Chodura<sup>11</sup> was based on a completely collisionless, ionization free model. Chodura’s work suggested that the magnetized presheath was subdivided into a region of flow along the magnetic field and a deflection region, after which the Bohm criterion is fulfilled for the normal component of the ion fluid velocity and the Debye sheath begins. Ahedo<sup>12</sup> offers an overview of different plasma-wall structures in the presence of a magnetic field, depending on the relative magnitudes of the three important scale lengths: the Debye length, the ion Larmor radius (given by  $r_{Li} = c_s / \omega$ ), and the collision mean free path. More recently, Riemann<sup>13</sup> presented a model of the same situation, but this time taking account of both collisions and ionization. We now present a simple fluid model of the presheath under the influence of a magnetic field, based on Riemann’s work.

## II. THE MODEL

### A. Geometry and approach

Consider a plasma in contact with an infinite planar boundary under the influence of a magnetic field at an oblique angle,  $\alpha$ , to that boundary. The wall is taken to be completely absorbing and planar as well as infinitely long. The latter implies that the electric field created by the wall’s charge is at right angles to it. It is convenient to define a coordinate system as follows: The origin lies at the point where all the fluid velocity components and the electric field are zero. This location will from hereon be referred to as the bulk plasma, although it may just as well be interpreted as the midplane of a symmetric system. The  $y$  axis is parallel to the wall, while the  $x$  axis is perpendicular to it (this is the direction of the electric field).  $\mathbf{B}$  lies entirely in the  $x$ – $y$  plane, which means that the  $z$  direction corresponds to the direction of  $\mathbf{E} \times \mathbf{B}$  (see Fig. 2).

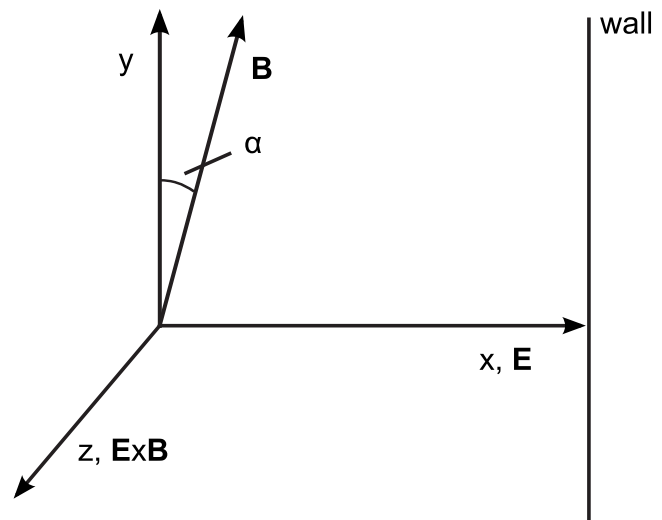


FIG. 2. The setup under consideration, as presented in Ref. 13.

### B. Theory

Assuming the ion fluid is one-dimensional and in steady state, the ion equation of motion and continuity equation are

$$m_i(\mathbf{v} \cdot \nabla)\mathbf{v} = e(\mathbf{E} + \mathbf{v} \times \mathbf{B}) - \frac{1}{n_i} \nabla p_i - m_i \nu_i \mathbf{v} \quad (1)$$

and

$$\nabla \cdot (n_i \mathbf{v}) = n_e \nu_i, \quad (2)$$

where  $\nu_i$  is the ionizing collision frequency,  $\nu_t$  is the total collision frequency (including ionization), and an ionization source term proportional to the electron density is included in Eq. (2). We assume uniform ion and electron temperatures,  $T_i$  and  $T_e$ , quasineutrality and the following equation of state for isothermal ions:

$$p_i = k_B T_i n_i. \quad (3)$$

We also assume that the electron density satisfies the Boltzmann relation,

$$n_i = n_e = n_0 \exp\left(\frac{eU}{k_B T_e}\right), \quad (4)$$

where  $U$  is the electrostatic potential and quasineutrality has been used. We define sets of dimensionless variables and parameters,

$$X = \frac{x}{\lambda_{mfp}}; \quad V = \frac{v}{c_s}; \quad \phi = -\frac{eU}{k_B T_e}, \quad (5)$$

$$\Delta = \frac{\nu_i}{\nu_t}; \quad \lambda_{mfp} = \frac{c_s}{\nu_t}; \quad \omega\tau = \frac{eB}{m_i \nu_t}, \quad (6)$$

where  $c_s = \sqrt{k_B(T_e + T_i)/m_i}$  is the ion acoustic speed,  $\omega$  is the ion gyrofrequency,  $\lambda_{mfp}$  is the ion collision mean free path (of ions travelling at  $c_s$ ),  $\tau$  is the associated collision time, and  $\Delta$  is the ratio of the ionization and total collision frequencies (from hereon referred to as “ionization ratio”). By combining Eqs. (1)–(4), separating the vector components of

the ion fluid velocity and using the normalizations given in Eqs. (5) and (6) one can obtain the following fluid equations:

$$V_x \frac{dV_y}{dX} = \omega\tau \sin(\alpha) V_z - V_y, \quad (7)$$

$$V_x \frac{dV_z}{dX} = \omega\tau \cos(\alpha) V_x - \omega\tau \sin(\alpha) V_y - V_z, \quad (8)$$

$$\left(V_x - \frac{1}{V_x}\right) \frac{dV_x}{dX} = -\omega\tau \cos(\alpha) V_z - \frac{\Delta}{V_x} - V_x, \quad (9)$$

$$V_x \frac{d\phi}{dX} = \frac{dV_x}{dX} - \Delta. \quad (10)$$

These equations determine the ion fluid velocities as well as the electrostatic potential in the presheath according to three free parameters:  $\Delta$ ,  $\alpha$ , and  $\omega\tau$ . These are, respectively, the ionization ratio, the magnetic field angle, and the ion Hall parameter. While the first two were defined earlier, the ion Hall parameter merits more explanation. It is the product of the gyrofrequency and the collision time of the ions and provides a measure of how magnetized the ions are. This parameter can span a vast range of values from  $10^{-3}$  in the Earth's magnetopause to  $10^6$  in tokamak fusion plasmas. Magnetron discharges, which are used in materials processing, usually have an ion Hall parameter between  $10^{-1}$  and 1. Upon closer examination of the left-hand side of Eq. (9), one notices a singular point at  $V_x=1$ . This corresponds to the sheath edge, where the assumption of quasineutrality breaks down and the space charge sheath begins. At this point the ion fluid fulfills the Bohm criterion (see Sec. I).

One can proceed either by setting  $\Delta$  and determining the presheath width from the calculation or vice versa. We adopt the earlier approach since the natural length scales of the presheath are of key interest in this work. To solve the equations of motion we use a polynomial substitution to obtain viable initial conditions for small  $X$ ,

$$\eta = \eta_1 X + \eta_2 X^3; \quad \eta = V_x, V_y, V_z, \quad (11)$$

$$\phi = \phi_1 X^2 + \phi_2 X^4. \quad (12)$$

The integration is then advanced using a Runge-Kutta method of sixth order with an adaptive step size, which requires that  $\Delta V_x < 10^{-5}$  for any given step. This enables us to closely approach the sheath edge singularity without incurring significant numerical errors. We terminate the integration when  $V_x \geq 1 - 10^{-4}$ , which immediately gives us  $X_{SE}$ .

### III. RESULTS

#### A. Presheath profiles

To gain a qualitative understanding of the impact of the magnetic field on the presheath it is useful to compare the profile of a collisional presheath with that of a magnetized one (Fig. 3). Both cases treat a magnetic field at an angle of  $\alpha=20^\circ$  with the wall and an ionization ratio of  $\Delta=1.0$ , but have  $\omega\tau=10^{-2}$  and  $10^2$ , respectively. This means that any differences in behavior are purely due to the fact magnetized

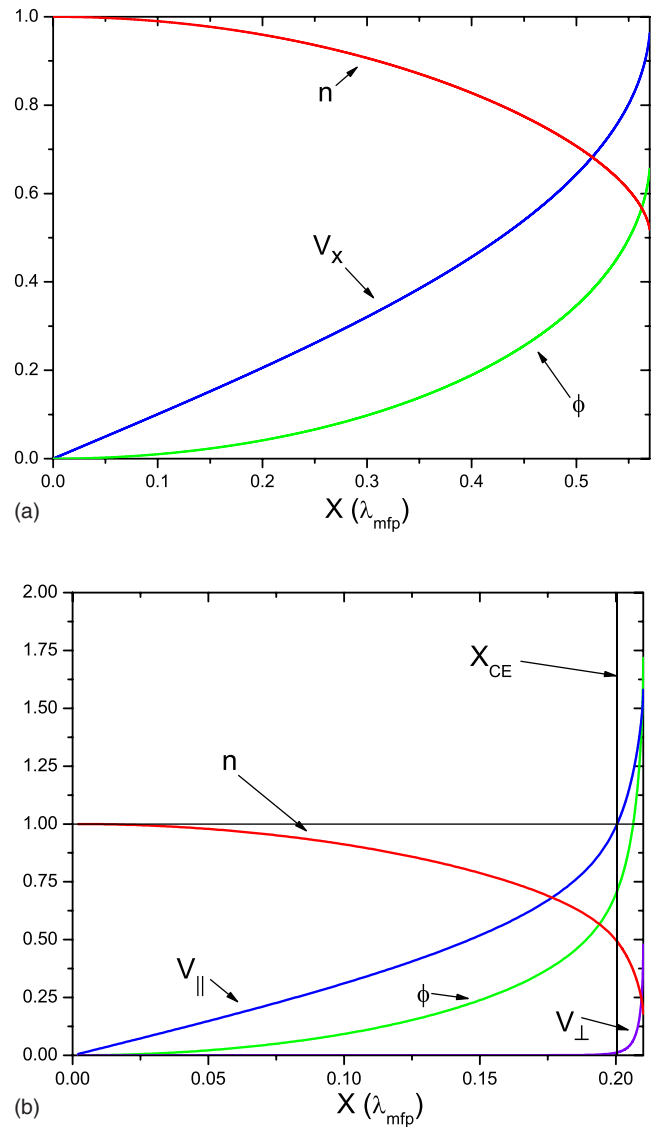


FIG. 3. (Color online) (a) Profile of the collisional presheath:  $\omega\tau=10^{-2}$ ,  $\alpha=20^\circ$ , and  $\Delta=1.0$ . (b) Profile of the magnetized presheath:  $\omega\tau=10^2$ ,  $\alpha=20^\circ$ , and  $\Delta=1.0$ .

flow and collisional transport across the field have been interchanged as the dominant physical effect on the ions in the presheath.

The collisional presheath (Fig. 3) and its behavior are already well documented. The wall perpendicular fluid velocity of the ions increases gradually across the entire width of the presheath, as does the potential causing this acceleration. The number density of both the ions and electrons decreases according to the electron Boltzmann relation [Eq. (4)]. Despite the fact that a magnetic field is still present ( $\omega\tau \neq 0$ ), the strong collisionality of the ion fluid enables it to diffuse across the field. This means that only a relatively weak electric field is required in the presheath to fulfill the Bohm criterion. At the sheath edge ( $X_{SE}=0.57\lambda_{mfp}$ ), the electrostatic potential takes a normalized value of 0.69 and the number density is 0.5. These correspond exactly to the values for a purely electrostatic ionization dominated presheath, according to Ref. 14.

This behavior is in contrast to that of the magnetized

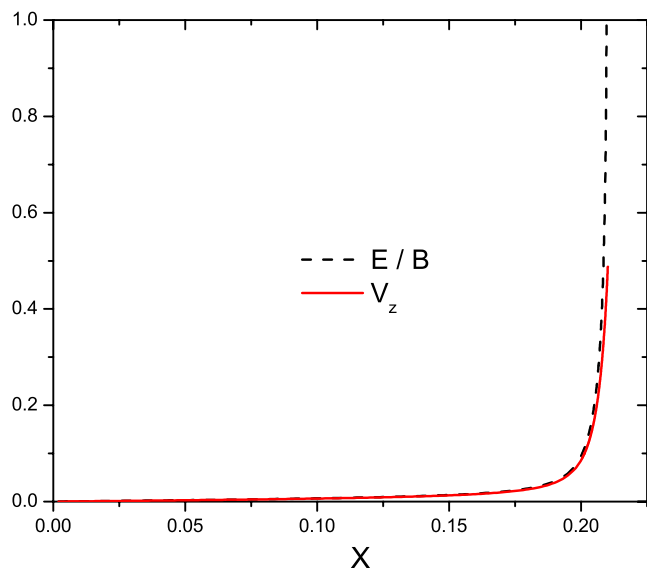


FIG. 4. (Color online) Profile of the quantity  $E/B$  and  $V_z$  for the magnetized presheath with  $\omega\tau=10^2$ ,  $\alpha=20^\circ$ , and  $\Delta=1.0$ .

presheath (Fig. 3). The magnetic field now dominates the ion motion in the presheath, so that it is convenient to resolve the fluid velocity parallel ( $V_{\parallel}$ ) and perpendicular ( $V_{\perp}$ ) to  $\mathbf{B}$  rather than using the coordinates defined earlier. Cross field transport is almost entirely suppressed up to  $X=X_{CE}$ , which is defined by the relation  $V_{\parallel}(X_{CE})=1$ . When dealing with plasma boundary problems one usually associates sonic flow with the breakdown of quasineutrality at the sheath edge. This was cause for debate, whether (super-) sonic flow along  $\mathbf{B}$  is permitted within the presheath. Such flow was found to be allowed, proof of which is summarized by Stangeby.<sup>15</sup>

It is helpful to consider the regions on either side of  $X=X_{CE}$  separately. When  $X<X_{CE}$ , the ion fluid is magnetized and the ion flow is parallel to the magnetic field. In fact, one can think of this region as an electrostatic, collisional presheath which has been aligned with the magnetic field. Hence we refer to this layer as the  $\mathbf{B}$ -aligned presheath or BAP. The potential and, by Eq. (4), the density have a profile which is nearly identical to that of a collisional presheath (Fig. 3) and exhibit the values normally associated with the sheath edge at  $X_{CE}$ .  $V_{\parallel}$  takes the place of  $V_x$ , except that there is no singularity associated with sonic flow in this direction.

For  $X>X_{CE}$  both magnetic and electrostatic forces play a significant role. The ion fluid is deflected from its flow along  $\mathbf{B}$  by a quickly rising electric field, such that the Bohm criterion is fulfilled at the sheath edge. This electric field also causes very strong flows to arise in the direction of  $\mathbf{E}\times\mathbf{B}$ . To determine how closely this flow corresponds to the  $\mathbf{E}\times\mathbf{B}$  drift velocity obtained from particle orbit theory, we plot a profile of the quantities  $E/B$  and  $V_z$  (Fig. 4). One can see that the velocities are very similar for most of the presheath, but  $E/B$  begins to diverge as we approach the sheath edge. In two-scale models this is simply due to the fact that the electric field is singular at the sheath edge. However, qualitatively similar results were obtained by Devaux *et al.* in an ion kinetic model of the magnetized, weakly collisional presheath.<sup>16</sup>

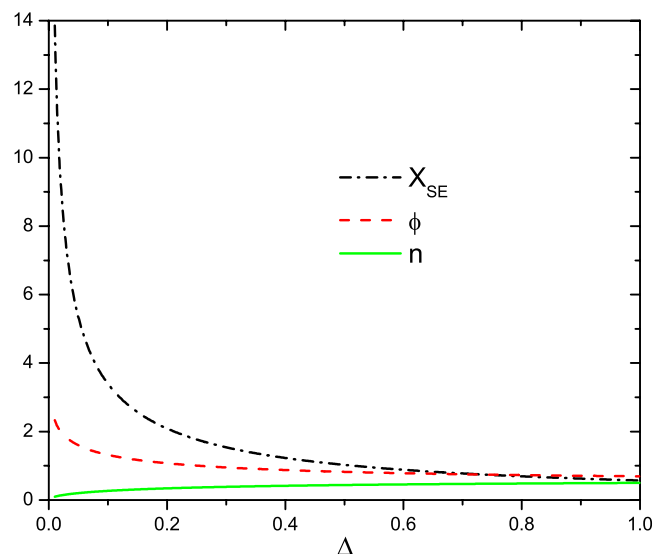


FIG. 5. (Color online) Variation of normalized sheath edge potential, number density, and presheath width [Eq. (5)] with  $\Delta$ , for  $\omega\tau=10^{-2}$ .

Existence of the deflection layer was originally proposed by Chodura<sup>11</sup> under somewhat different conditions, using the term “magnetic sheath.” This is perhaps a misnomer, since he refers to a region within the quasineutral presheath. In his treatment there was no account of either collisions or ionization, which would correspond to the limit of  $\omega\tau\rightarrow\infty$  in terms of the parameters used here. In his description this layer (from hereon we will refer to the area defined as  $X>X_{CE}$  as the “Chodura layer”, rather than “magnetic sheath”) is separated from the BAP by a discontinuity at  $V_{\parallel}=1$ . While it may seem that Chodura’s results have little relevance to a plasma which has both ionization and collisions we find that for high Hall parameters the qualitative behavior of the plasma beyond  $X_{CE}$  corresponds very closely to that outlined by Chodura.

## B. The ionization and Hall parameters

The ionization ratio,  $\Delta$ , has a significant effect on the presheath width, as well as the density and electrostatic potential. This relates to the fact that the Bohm criterion must be fulfilled at the sheath edge, regardless of how frequent ionizing collisions are in the presheath. To balance the ion wall losses, one requires a far larger presheath if the ionization rate is low. The sheath edge number density is reduced, as the losses have greater impact on the presheath and the potential at this point is adjusted accordingly (Fig. 5). Qualitatively, this behavior is the same in both the magnetized and collisional presheath. The fluid velocities at the sheath edge are completely unaffected by changes in  $\Delta$  in a collisional situation and even at high  $\omega\tau$  only vary slightly. The wall normal component is, of course, still the Bohm velocity while the velocity in the  $\mathbf{E}\times\mathbf{B}$  direction rises slightly with high  $\Delta$  (and a correspondingly compact presheath) due to the steeper potential gradient near the sheath edge. Wall parallel flow is reduced, as the fluid spends less time being accelerated along the magnetic field.



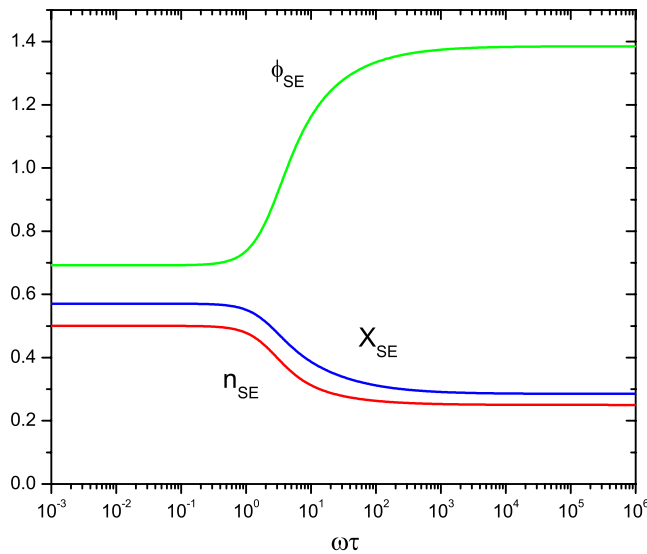


FIG. 6. (Color online) Variation of normalized sheath edge potential, number density, and presheath width with  $\omega\tau$ .

In an attempt to characterize the effects of the magnetic field on the presheath, we identify two limiting regimes of the Hall parameter. This can be done by examining the variation of the sheath edge values of the presheath parameters with  $\omega\tau$ . Figure 6 shows how the potential and density at the sheath edge as well as the sheath edge's location vary as  $\omega\tau$  increases from  $10^{-3}$  to  $10^6$ . The transition from the collisional to the magnetized regime occurs in the range  $10^{-1} < \omega\tau < 10^2$ , outside of which the parameters vary only slightly with further changes in the Hall parameter.

### C. The field angle and scale lengths

As mentioned before, the Chodura layer serves to deflect the ion fluid from the magnetic field direction and divert it such that the Bohm criterion is fulfilled at the sheath edge. This deflection has to be larger for smaller values of  $\alpha$ , which would suggest that the Chodura layer has to be more pronounced. Figure 7 shows the angle,  $\beta$ , the ion fluid velocity in the  $x$ - $y$  plane makes with the wall, plotted against  $\alpha$ . The solid lines refer to values taken at the sheath edge, while the dashed lines are taken at the boundary between the BAP and the Chodura layer (the Chodura edge). As  $\omega\tau$  is increased, the ion flow aligns with the magnetic field. This can be seen in the tendency of the dashed lines towards the limiting case where  $\beta = \alpha$ . For any given  $\omega\tau$  there is a magnetic field angle for which the deflection occurring in the Chodura layer is maximized. This angle gradually shifts towards zero as the Hall parameter is increased. However, when  $\alpha = 0$ , there is no more fluid flow along the magnetic field. In this case one has to solve a diffusion problem, as collisions are now the only means of supplying ions to the sheath.

One way of judging whether a magnetized presheath is likely to form a Chodura layer of non-negligible size is to determine the field parallel ion fluid velocity at the sheath edge. While the condition for entry into this layer is sonic flow along  $\mathbf{B}$ , it is only when  $V_{\parallel}(X_{SE}) > 1.2$  that significant

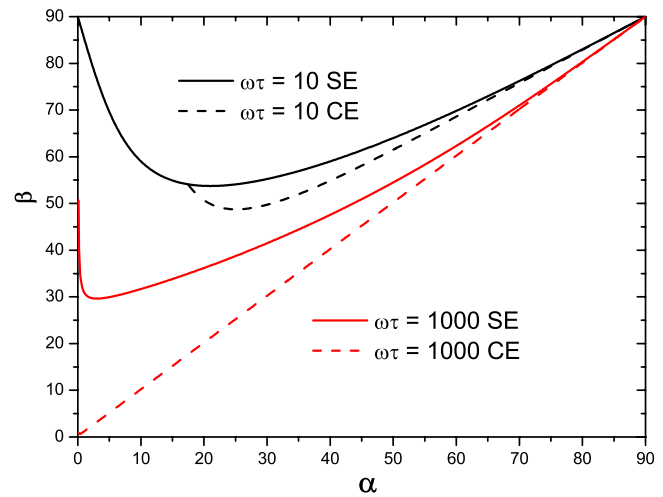


FIG. 7. (Color online) The angle of the ion fluid velocity with the wall (measured in the  $x$ - $y$  plane),  $\beta$ , against  $\alpha$  for different  $\omega\tau$ . Solid lines refer to values taken at the sheath edge, while dashed ones refer to the Chodura edge. Note that the ion flow in the BAP is only fully aligned with the magnetic field for sufficiently high  $\omega\tau$ .

acceleration occurs within the Chodura layer. Judging from Fig. 8 this occurs for field angles between  $5^\circ$  and  $50^\circ$ . This is only a rough estimate of the relevant parameter range, but the following results will show that it agrees rather well with other properties of the Chodura layer.

In order to characterize the highly magnetized presheath, we attempt to determine appropriate scale lengths for the BAP and the Chodura layer. In Sec. III A the BAP was described as a collisional presheath, aligned with the magnetic field. One can imagine it as the purely electrostatic case, turned through an angle  $\alpha$ . Thus, we expect the quantity

$$L_{BAP} = \frac{X_{SE}}{\sin(\alpha)} \quad (13)$$

to be independent of  $\alpha$ . The extent of the Chodura layer is negligible on this scale, provided  $\omega\tau$  is sufficiently large. This layer serves to deflect the ion fluid from the direction of the magnetic field. Chodura<sup>11</sup> suggested that the layer would

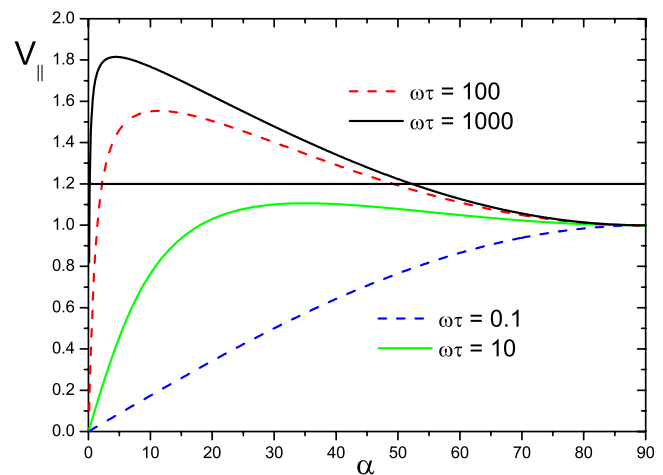


FIG. 8. (Color online) Ion fluid velocity parallel to  $\mathbf{B}$  at the sheath edge against  $\alpha$ , for various values of  $\omega\tau$ .

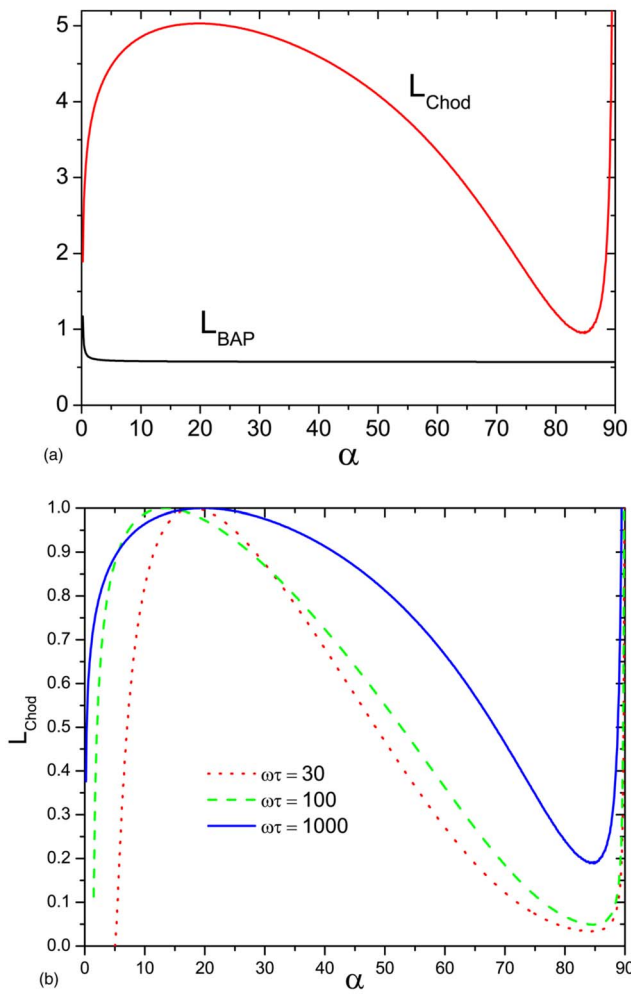


FIG. 9. (Color online) (a) Variation of the length of BAP and Chodura layer with  $\alpha$ , for  $\omega\tau=10^3$  and  $\Delta=1$ . (b) Variation of the length of the Chodura layer with  $\alpha$ , for  $\omega\tau=30, 10^2, 10^3$  and  $\Delta=1$ .

scale with the Larmor radius of ions travelling at the acoustic speed,  $r_L = c_s / \omega$ . Chodura concluded that the layer width is  $\sqrt{6}r_L \cos \alpha$ . Here we simply define

$$L_{\text{Chod}} = \frac{X_{\text{SE}} - X_{\text{CE}}}{\cos(\alpha)} \left( \frac{\lambda_{\text{mfp}}}{r_L} \right), \quad (14)$$

which is the Chodura layer width normalized to units of  $r_L$  with a factor of  $\cos(\alpha)$  included.

Figure 9(a) shows  $L_{\text{BAP}}$  and  $L_{\text{Chod}}$  plotted against  $\alpha$  for  $\omega\tau=10^3$  and  $\Delta=1$ . As expected, we see that  $L_{\text{BAP}}$  is independent of  $\alpha$ , except for magnetic field angles in the range  $\alpha < 10^\circ$ . The scale length tends towards zero when the angle becomes small, so it is not surprising that  $L_{\text{BAP}}$  begins to diverge. The Chodura layer's equivalent lies in the correct order of magnitude, but does not contain the exact functional dependence of  $L_{\text{Chod}}$  on  $\alpha$ .

We can attribute the discrepancy between the model presented here and the original one by Chodura to his neglect of collisions. Inclusion of collisions facilitates the redirection of the ion flow away from the magnetic field and towards the wall. One might therefore expect the Chodura layer to be smaller than predicted. To examine this, we obtain data for

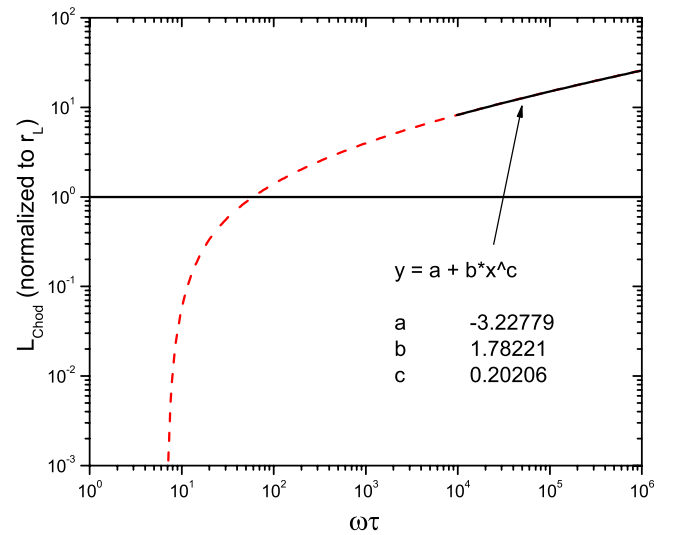


FIG. 10. (Color online) Width of the Chodura layer, plotted against  $\omega\tau$  on a log-log scale; normalized to  $r_L$ . The dashed black line is a power law fit, for  $\omega\tau > 10^3$ . From the resulting parameter,  $c$  we conclude that  $L_{\text{Chod}} \propto (\omega\tau)^{0.202}$ .

the quantity  $L_{\text{Chod}}$ , plotted in Fig. 9(b) for different Hall parameters. For each value of  $\omega\tau$  we divide the data set by its maximum value, such that the curves can be plotted against  $\alpha$  on the same scale. The resultant graphs are given in Fig. 9. One can see that as  $\omega\tau$  is increased, the dependence of  $L_{\text{Chod}}$  on  $\alpha$  becomes flatter, i.e., closer to the uniform value of unity one would expect from Chodura's result.<sup>11</sup> If we were to take the limit of  $\omega\tau \rightarrow \infty$ , one would find that Eq. (14) gives the correct scaling. Finally, it is noteworthy that this scale length also has a divergence as  $\alpha \rightarrow 90^\circ$ . Furthermore, the Chodura layer width determined from these calculations becomes small for nearly wall parallel fields. When  $\alpha \rightarrow 0$ , there is no fluid flow along the field and the treatment outlined in Sec. II does not apply.

## D. Pseudo two-scale magnetized presheath

As the Hall parameter increases, so does the normalized width of the Chodura layer (Fig. 10). This is another indication that the limiting behavior for high Hall parameters is akin to the problem described by Chodura.<sup>11</sup> In Chodura's treatment, the lack of ionization in the "magnetic sheath" meant that the layer was semi-infinite. In this model, the width of the Chodura layer continues to increase steadily past  $\omega\tau=10^2$  (which marks the boundary of the magnetized regime). The gradient of  $L_{\text{Chod}}$  on the log-log scale becomes constant when  $\omega\tau > 10^4$ , which would imply that the layer continues to grow without limit. The dependence of  $L_{\text{Chod}}$  on  $\omega\tau$  can be determined using a power law fit. We find that it obeys the following relation with good accuracy:

$$L_{\text{Chod}} \propto (\omega\tau)^{0.202}. \quad (15)$$

However, if one tracks the same limiting behavior on the scale of the whole presheath or the BAP (which are both related to  $\lambda_{\text{mfp}}$ ), then the Chodura layer is at its largest when the criteria for its creation are only just fulfilled. As the Hall parameter is increased further, the extent of the Chodura

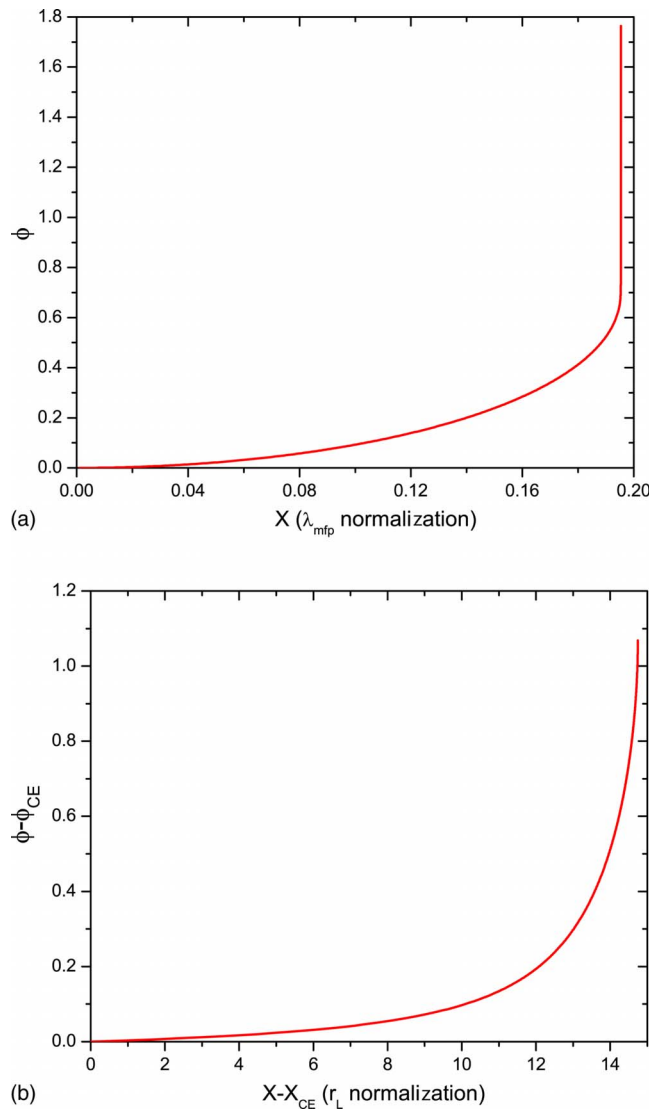


FIG. 11. (Color online) (a) Profile of the presheath for  $\omega\tau = 10^5$ , plotted on the collision mean free path scale. (b) Profile of the Chodura layer for the same  $\omega\tau$  on the Larmor radius scale. Both figures have  $\alpha = 30^\circ$ .

layer decreases, because  $r_L$  decreases. It vanishes as  $\omega\tau \rightarrow \infty$ . This means that in the limit of large  $\omega\tau$  it is possible to recover the two-scale behavior of a magnetized presheath outlined by Chodura.<sup>11</sup> In fact, it is possible to make use of this when solving the equations of motion numerically. Upon entering the Chodura layer one normally has to deal with very steep gradients in the velocities and the potential, which calls for a very small step size. By renormalizing the equations to the Larmor radius length scale at the Chodura edge one can keep the contributions in each step in the calculations larger, which reduces the computational errors associated with very small numbers. It is therefore possible to resolve the behavior in the Chodura layer in far greater detail than would be possible otherwise. Figure 11 shows a highly magnetized presheath's potential, plotted on the scale of the BAP and the Chodura layer. This demonstrates the effectiveness of the pseudo two-scale approach in resolving the Chodura layer in detail.

#### IV. CONCLUSIONS

This work applies a one-dimensional fluid model to a plasma in contact with an infinite planar boundary under the influence of a magnetic field at an oblique angle to that boundary. Using the symmetry of the problem one can simplify it to a set of four coupled first order differential equations. These are fully determined by three parameters:  $\alpha$  (the angle between the magnetic field and the wall),  $\Delta$  (ratio of the ionization and total collision frequencies), and  $\omega\tau$  (the ion Hall parameter). The equations are integrated numerically, starting from a position close to the bulk plasma, where the electric field is zero. The integration is terminated when the Bohm criterion is fulfilled.

We identify two different regimes of magnetization ( $\omega\tau < 0.1$ ,  $\omega\tau > 10^2$ ), in which the sheath edge parameters are insensitive to changes in the Hall parameter. When the plasma is highly magnetized ( $\omega\tau > 10^2$ ), the magnetized plasma boundary can be described in terms of three regions. Approaching the wall from the bulk plasma ( $E=0$ ), we have the BAP (*B*-aligned presheath), the Chodura layer, and the Debye sheath. In the Chodura layer, the electric field becomes strong enough to deflect ions from their magnetized flow in the BAP. This must be done in order to fulfill the Bohm criterion at the sheath edge. We use the term Chodura layer in recognition of qualitative similarities with the magnetized presheath ("magnetic sheath") described by Chodura,<sup>11</sup> although the present analysis is based on different assumptions. Hence, a well developed Chodura layer can only form for certain parameters in our model, namely, high  $\omega\tau$  and field angles in the range  $5^\circ < \alpha < 50^\circ$ . The layer as it was originally described can be recovered in the limit  $\omega\tau \rightarrow \infty$ , as demonstrated for very high Hall parameters by resolving both scale lengths using a pseudo two-scale approach.

This model relies on several assumption, which leaves room for generalization. For example, the ions are assumed to be isothermal, such that the acoustic speed is constant. One can also apply these calculations when  $T_i$  is far less than  $T_e$ , in which case isothermal ions are no longer required. The fluid model presented here could be extended to apply to finite systems and more complicated geometries, to model real situations. As for applications, one might consider a magnetron discharge or the divertor region of a tokamak. The potential distribution obtained from these calculations could, for example, be used to determine the dynamics of dust grains (solid particles in the plasma) in such an environment. Alternatively, one could attempt to apply some of the theory to charge collection by a probe or dust grain in a magnetized plasma. On the other hand, a kinetic treatment of the problem would yield more accurate results, but such an analysis is difficult and in many cases hardly possible. Devaux *et al.* presented an ion kinetic model of the magnetic presheath,<sup>16</sup> which would provide a good reference point on the way to generalizing a code to deal with problems in more complicated geometries. It would also be advisable to reassess the applicability of the Boltzmann relation for electrons to the magnetized case.<sup>17,18</sup>



- <sup>1</sup>I. Langmuir, *Gen. Electr. Rev.* **26**, 731 (1923).  
<sup>2</sup>I. Langmuir, *Proc. Natl. Acad. Sci. U.S.A.* **14**, 627 (1928).  
<sup>3</sup>R. N. Franklin, *J. Phys. D* **36**, R309 (2003).  
<sup>4</sup>R. N. Franklin, *J. Phys. D* **38**, 3412 (2005).  
<sup>5</sup>S. O. Cetiner, Ph.D. thesis, University of London, 2005.  
<sup>6</sup>A. Caruso and A. Cavaliere, *Nuovo Cimento* **26**, 1389 (1962).  
<sup>7</sup>K.-U. Riemann, *Plasma Phys. Controlled Fusion* **47**, 1949 (2005).  
<sup>8</sup>L. Tonks and I. Langmuir, *Phys. Rev.* **34**, 876 (1929).  
<sup>9</sup>D. Bohm, *Characteristics of Electrical Discharges in Magnetic Fields* (McGraw-Hill, New York, 1949).  
<sup>10</sup>E. R. Harrison and W. B. Thompson, *Proc. Phys. Soc. London* **74**, 145 (1959).  
<sup>11</sup>R. Chodura, *Phys. Fluids* **25**, 1628 (1982).  
<sup>12</sup>E. Ahedo, *Phys. Plasmas* **4**, 4419 (1997).  
<sup>13</sup>K.-U. Riemann, *Contrib. Plasma Phys.* **34**, 127 (1994).  
<sup>14</sup>P. C. Stangeby, *The Plasma Boundary of Magnetic Fusion Devices* (Institute of Physics, Bristol, 2000).  
<sup>15</sup>P. C. Stangeby, *Phys. Plasmas* **2**, 702 (1995).  
<sup>16</sup>S. Devaux and G. Manfredi, *Phys. Plasmas* **13**, 083504 (2006).  
<sup>17</sup>N. Sternberg, V. Godyak, and D. Hoffman, *Phys. Plasmas* **13**, 063511 (2006).  
<sup>18</sup>J. E. Allen, *Book of Abstracts, 7th International Workshop on Electrical Probes in Magnetised Plasmas*, Prague, 2007, edited by Milan Tichý, Pavel Kudrna, and Vitezslav Stranak (Matfyz Press, Prague, 2007), p. 32.